Tuning of fluorescence efficiency via local modification of the crystal structure by benzyl groups in polymorphism of a pyrazine dye

Yoko Akune[1], Risa Hirosawa[1], Natsuko Endo[1], Sayumi Hatano[1], Takuya Hosokai[2], Hiroyasu Sato[3] and Shinya Matsumoto[1,*]

[1]Graduate School of Environmental and Information Sciences, Yokohama National University, 79-7 Tokiwadai, Hodogaya-ku, Yokohama 240-8501, Japan

[2]National Institute of Advanced Industrial Science and Technology, 1-1-1 Umezono, Tsukuba, 305-8568 Japan

[3]X-ray Research Laboratory, Rigaku Corporation,
3-9-12 Matsubaracho, Akishima, Tokyo 196-8666, Japan

[*]Corresponding author. Tel.: +81-45-339-3366; fax: +81-45-339-3345. E-mail address: smatsu@ynu.ac.jp (Shinya Matsumoto).

Abstract

Polymorphism-dependent fluorescence, a phenomenon in which a compound shows various fluorescence properties among its polymorphs, contributes to understanding the relationship between the crystal structure and solid-state fluorescence properties. Here we report that a variety of solid-state fluorescence efficiency by benzyl groups based on polymorphs in an organic pyrazine dye where the polymorphs showed quite different fluorescence efficiency (fluorescence quantum yield: 14% vs 64%) despite their similar molecular conformations and packing motifs in the crystal structures. Crystal structure analysis and optical measurements revealed local loose packing caused by the benzyl groups, which are not a part of the pyrazine fluorophore, greatly influenced fluorescence efficiency in the polymorphs. This result showed that a benzyl substituent can be used as an effective molecular modification for tuning solid-state fluorescence efficiency.

Keywords

Polymorphism, solid-state fluorescence efficiency, benzyl group, loose packing, 2,5-diamino-3,6-dicyanopyrazine dye

1. Introduction

Tuning of solid-state photoluminescence properties is key to developing organic functional materials such as light-emitting diodes, solar cells, and memory devices.[1] Various studies have reported the tuning of solid-state photoluminescence properties using molecular modification and various solvate formations.[2] Recently, polymorphism-dependent fluorescence, a phenomenon in which a compound shows various fluorescence properties among its polymorphs, has attracted much attention in academic and industrial research.[3] Polymorphism is defined as the ability of a compound to exhibit two or more crystal forms.[4] Physicochemical properties vary among polymorphs due to their different crystal structures.[5] Understanding polymorphism-dependent fluorescence involves clarifying the relationship between crystal structure and fluorescence properties. Furthermore, polymorphs can transform into other polymorphs under external stimulus.[6] As such, compounds with polymorphs are expected to be applied to novel functional materials, such as sensors and switched, utilizing this stimuli responsiveness.[7]

Compounds reported as showing polymorphism-dependent fluorescence can be divided into two groups based on the type of polymorphism: conformational or packing. As a definition, conformational polymorphism results in both different molecular conformations and molecular arrangements in the crystal polymorphs, whereas packing polymorphism only results in different molecular arrangements.[4] Polymorphism-dependent fluorescence in conformational polymorphs has been mainly reported for aggregation-induced emission (AIE) compounds.[8] These studies have indicated that the introduction of a rotationally flexible substituent, such as a phenyl group, into a fluorophore is a sufficient molecular modification to realize polymorphism-dependent fluorescence. However, conformational polymorphism employing flexible substituents makes understanding the effect of crystal structure on fluorescence properties, particularly fluorescence efficiency, more complicated. Packing polymorphism with various fluorescence properties is optimal for understanding structure-property relationships, although the structural differences among the polymorphs were strongly correlated with the mother structure of the compound.[3a–b] In other words, molecular modifications that can be applied to various well-known fluorophores in the conformational polymorphism[9] have yet to be sufficiently established in the packing polymorphism. Therefore, to understand structure-property relationships in solid-state fluorescence properties, and develop novel functional materials, it is necessary to realize polymorphism-dependent fluorescence in packing polymorphism via a simple molecular modification. Herein, we report the packing polymorphism of a 2,5-bis[*N*,*N*-di-(4-chlorophenyl)methylamino]-3,6-

dicyanopyrazine dye (**1**, Fig. 1), which showed quite different fluorescence efficiencies between two polymorphs: a new polymorph with orange weak fluorescence and a previously reported polymorph with intense yellow fluorescence.[10] The results of crystal structure analysis indicated that the benzyl groups, which were not a part of the fluorophore of **1**, played an essential role in tuning the fluorescence efficiency between the polymorphs via local modification of the crystal packing. This finding suggested that the introduction of benzyl groups to fluorophores can be an effective strategy for obtaining a compound with various solid-state fluorescence properties.

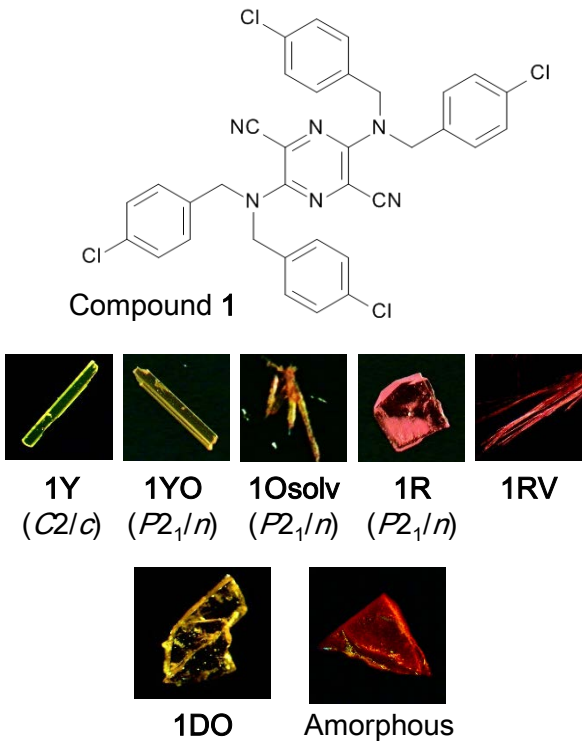

Figure 1. Structure of compound **1** and its seven solid forms, including an amorphous solid.

2. Experimental

2.1. Material

Compound **1** was supplied by Nippon Soda Co. Ltd. The synthesis of **1** is described in our previous study.[11]

2.2. Crystallization

One crystal form (**1DO**) of **1** was newly obtained in addition to the previously reported five crystal

forms (**1Y**, **1YO**, **1Osolv**, **1R**, and **1RV**),[10] where **Y**, **YO**, **DO**, **Osolv**, **R**, and **RV** represent the colors of the respective crystals: yellow, yellowish orange, dark orange, orange solvate, red, and reddish violet. The crystal structures of **1Y**, **1YO**, **1Osolv** and **1R** were reported.[10-12] In this study, the X-ray diffraction measurements of **1DO** and **1RV** were performed.

An X-ray diffraction-quality crystal of **1DO** was obtained using the liquid-liquid diffusion method from $CHCl_3$/*n*-hexane. An X-ray diffraction-quality crystal of **1RV** was using a mixed solution of $CHCl_3$ and *n*-hexane.

2.3. X-ray analysis of **1DO** and **1RV**

Diffraction data for **1DO** were collected at 296 K on a Rigaku R-AXIS Rapid diffractometer using graphite-monochromated Cu-*K*α radiation (λ = 1.54187 Å). The numerical absorption correction for **1DO** was applied using RAPID-AUTO.[13] The structures of **1DO** were solved and refined using SIR2004[14] and SHELXL97[15] respectively. Diffraction data for **1RV** were collected at 93 K on a Rigaku XtaLAB P200 using graphite-monochromated Cu-*K*α radiation (λ = 1.54187 Å). Absorption correction for **1RV** was performed by a multiscan using CrysAlisPro 1. 171. 39. 7e.[16] The structures of **1RV** were solved and refined using SHELXT.[17] All nonhydrogen atoms in **1DO** and **1RV** were anisotropically refined by a full-matrix least-squares refinement based on F^2. Hydrogen atoms in the two forms were located at the calculated positions and refined using the riding model. Publication materials were generated by CrystalStructure 4.2[18] and Mercury 3.8.[19]

2.4. Thermal measurement and the preparation of an amorphous solid

Differential scanning calorimetry (DSC) was conducted in crimped aluminum pans using a Rigaku Thermo plus2 DSC8230 at a heating rate of 10 K min^{-1}. An amorphous solid form of **1** was prepared by rapid cooling of molten **1**. The solid was characterized by powder X-Ray diffraction, giving no diffraction peak (Fig. S1). Powder X-ray diffraction was performed using the same Rigaku R-AXIS Rapid diffractometer as for single crystal X-ray diffraction at room temperature. Measurements were conducted in the 2θ range from 5° to 40°.

2.5. Optical measurements

Absorption and emission spectra of **1Y**, **1Osolv** and **1** in $CHCl_3$ solution have been reported previously,[10] although the detailed analysis of fluorescence properties using photoluminescence

lifetime data were not carried out. The absorption spectra of **1DO**, **1R**, **1RV**, and an amorphous solid were corrected using a SIS-50 surface and interface spectrometer based on optical waveguide spectroscopy (System Instruments). The absorption spectrum of **1YO** was not measured because of the lack of sufficient amount of sample. The fluorescence spectra of **1DO**, **1R**, **1RV**, and an amorphous solid were recorded on a FP-8500 fluorometer (JASCO) and quantum yields were determined using an integrating sphere unit. These measurement sets were the same as those of **1Y** and **1Osolv**, which have been reported previously.[10]

The photoluminescence lifetimes of **1DO**, **1Y**, **1R**, and an amorphous solid were determined using a Fluoro Cube fluorescence lifetime system (HORIBA). The excitation wavelength was 455 nm, and emission was monitored at 564 nm for **1DO**, 558 nm for **1Y**, 607 nm for **1R**, and 615 nm for an amorphous solid.

Fourier transform infrared (FTIR) spectra of single crystals (**1DO** and **1Y**) or an amorphous solid were obtained by microscopic transmittance method using a FT/IR-6200typeA (JASCO).

3. Results and Discussion

3.1. New polymorph of **1**

In a previous study, we reported five crystal forms of compound **1** with different colors, namely **1Y**, **1YO**, **1Osolv** (benzene solvate), **1R**, and **1RV**, and their crystal structures were determined by single crystal X-ray diffraction analysis, except for that of **1RV**.[10-12] These polymorphs had different conformations, representing conformational polymorphism (Fig. S2). In this study, crystals of a new polymorph with a dark orange color (**1DO**) were serendipitously obtained from combined solvent $CHCl_3$/*n*-hexane, despite this solvent combination usually producing a yellow form (**1Y**), which is more thermally stable (Fig. 1).[12] The powder pattern of **1DO** was different from those of the other five crystal forms, and so **1DO** was regarded as a new polymorph of this dye (Fig. 2). Thermal observation using differential scanning calorimetry characterized **1DO** as a thermally metastable form that transformed into **1Y**, with an exothermic peak, upon heating (Fig. S3). Single crystal X-ray diffraction analysis of **1DO** (Table 1) revealed that the molecular conformations of **1DO** and **1Y** were similar (Fig. S4, Table S1), demonstrating that **1DO** and **1Y** showed packing polymorphism.

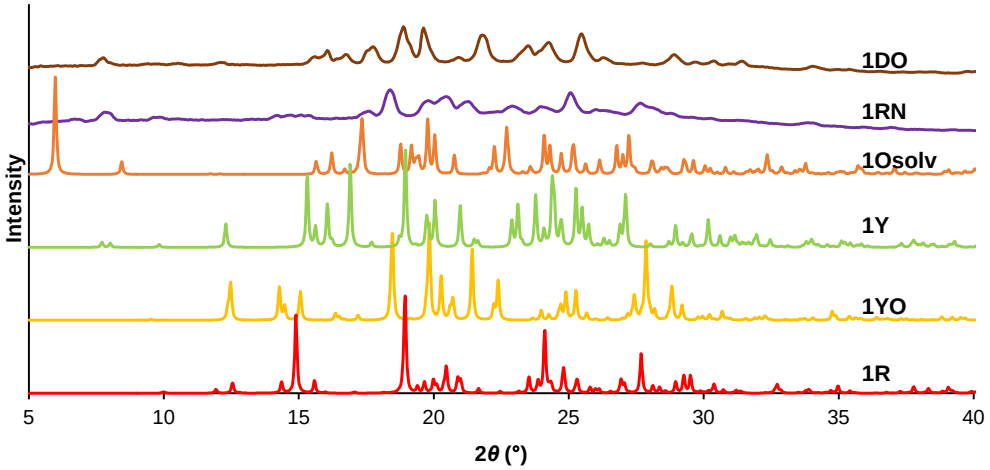

Figure 2. XRD patterns of the six crystal forms of **1**. The crystal structures of four forms, **1Y**, [10] **1YO**, [10] **1Osolv**, and **1R**,[10] were solved by single-crystal X-ray diffraction analysis, and patterns were simulated using the atomic coordinates obtained by X-ray analysis. Powdered **1DO** was obtained from $CHCl_3$/*n*-hexane. Powdered **1RV**[10] was obtained using a mixed solvent solution of $CHCl_3$ and *n*-hexane.

Table 1. Crystallographic information for six forms of **1**.

Derivatives	**1DO**	**1Y**[11]	**1YO** [12]	**1Osolv**[10]	**1R** [11]	**1RV**
Formula	$C_{34}H_{24}N_6Cl_4$	$C_{34}H_{24}N_6Cl_4$	$C_{34}H_{24}N_6Cl_4$	$C_{34}H_{24}N_6Cl_4\cdot 2C_6H_6$	$C_{34}H_{24}N_6Cl_4$	$C_{34}H_{24}N_6Cl_4$
Formula weight	658.42	658.42	658.42	814.64	658.42	658.42
Space group	$P2_1/n$	$C2/c$	$P2_1/n$	$P2_1/n$	$P2_1/n$	$P2_1/c$
T (K)	296	296	296	93	296	93
a (Å)	14.6554(5)	23.485(5)	7.6803(13)	15.9806(19)	9.441(2)	4.70709(16)
b (Å)	6.00711(18)	5.974(1)	18.549(4)	5.8569(7)	11.084(2)	26.1213(12)
c (Å)	17.9996(5)	22.593(7)	11.229(3)	22.172(3)	15.303(3)	12.1528(5)
α (°)	90	90	90	90	90	90
β (°)	90.1994(14)	102.69(1)	92.71(2)	109.263(8)	104.380(9)	93.267(3)
γ (°)	90	90	90	90	90	90
Z	2	4	2	2	2	2

V (Å^3)	1584.62(8)	3092.3(1)	1597.9(6)	1959.0(5)	1551.1(5)	1491.82(11)
D_{calc} (g/cm^3)	1.380	1.414	1.368	1.381	1.410	1.466
F (000)	676	1352	676	844	676	676
μ (mm^{-1})	3.669	3.760	3.639	3.079	3.748	3.897
No. of reflns collection	13776	13712	10621	3490	14137	8347
No. of unique reflns /parameters	2751/200	2618/211	2712/199	3490/271	2818/211	2970/199
R1/wR2	0.0762/ 0.2408	0.0470/ 0.0620	0.0650/ 0.1694	0.0556/ 0.1550	0.0470/ 0.1190	0.0567/ 0.1793
GOF	1.606	1.279	1.089	1.015	1.062	1.096
CCDC number	1525754	600795	1402481	1479193	600794	1525752

3.2. Optical properties of polymorphs of **1DO** and **1Y**

The color differences among the conformational polymorphs of compound **1** (**1Y**, **1R**, and **1Osolv**) originated from molecular deformation in terms of the amino groups.[10,11] This indicated that the electronic transition of **1DO** in the visible region was probably the same as that of **1Y**, owing to their almost identical molecular conformations (Fig. S4). This hypothesis was supported by similarities between the absorption and fluorescence spectra of **1DO** and **1Y** (Figs. 3 and S5). In contrast, the fluorescent quantum yield of **1DO** was markedly lower than that of **1Y**, at 14% and 64%,[10] respectively. The fluorescence decay processes between **1DO** and **1Y** were also different. The fluorescence lifetime of **1DO** (4.9 ns) was much shorter than that of **1Y** (22.4 ns), whereas the non-radiative decay rate of **1DO** (17.7×10^7 s^{-1}) was larger than that of **1Y** (1.6×10^7 s^{-1}), despite the radiative decay rates of these two polymorphs being the same (Table 2). The differences in intermolecular interactions caused by distinctive molecular arrangements would have a great impact on the fluorescence efficiencies of the two polymorphs.

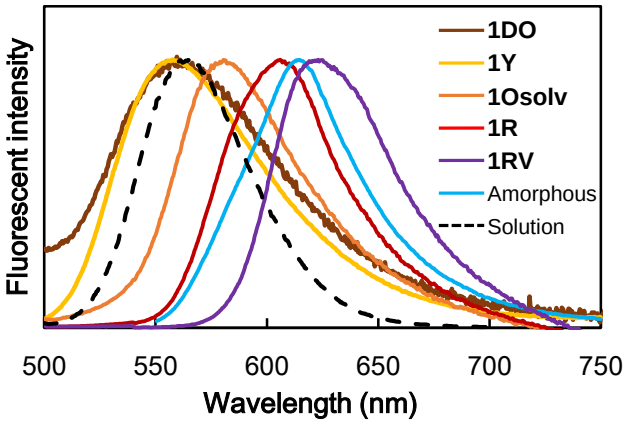

Figure 3. Fluorescence spectra of **1DO**, **1Y**, **1Osolv**, **1R**, **1RV**, an amorphous solid of **1**, and a chloroform solution of **1**.

Table 2. Absorption and fluorescence parameters of the polymorphs and an amorphous solid of **1**.

	Absorption	**Emission**	**Quantum yield**	**Lifetime**	**Decay rate**	
	λ_{max} **(nm)**	F_{max} **(nm)**	Φ **(%)**	τ **(ns)**	k_f **(s^{-1})**[a]	k_{nr} **(s^{-1})**[b]
1DO	484	561	14	4.9	2.9×10^7	17.7×10^7
1Y	484[10]	558[10]	64[10]	22.4	2.9×10^7	1.6×10^7
1YO[c]	N. A.	N. A.	N. A.	N. A.	N. A.	N. A.
1O$_{solv}$	508[10]	581[10]	52[10]	N. A.[d]	N. A.[d]	N. A.[d]
1R	554	606	78	60.0	1.3×10^7	0.4×10^7
1RV	593	623	37	N. A.[c]	N. A.[c]	N. A.[c]
Am[e]	490	615	79	16.5	4.8×10^7	1.3×10^7

[a] k_f represents the radiative decay rate, calculated using the equation, $k_f = \Phi/\tau$.

[b] k_{nr} represents the non-radiative decay rate, calculated using the equation, $k_{nr} = 1/\tau - k_f$.

[c] The measurements were not carried out because of the lack of sample amounts.

[d] The measurement was not carried out because the powder of **1Osolv** was in a wet state by benzene solvent and it was very difficult to maintain the stability of **1Osolv** at room temperature.

[e] Am represents an amorphous solid.

3.3. Relationship between crystal structures and fluorescent efficiency

To evaluate the effects of intermolecular interactions on the fluorescence efficiency, we examined the relationship between fluorescent quantum yield and fluorophore packing in the crystal structures of

1DO and **1Y**, in addition to the other three polymorphs showing intense fluorescence (**1Osolv**: 52%,[10] **1R**: 78%, and **1RV**: 37%). The evaluation was included the benzene solvate form of **1**, **1Osolv**, because the crystal structure of **1Osolv** was similar to that of **1Y** in terms of the fluorophore packing,[10] that is, the benzene molecules in the crystal structure of **1Osolv** are considered to have insignificant impact on the formation of fluorophore packing which would be correlated to fluorescence efficiency. The fluorescence quantum yields were in correlation with the distances between the centers of gravity in the fluorophore, except for **1DO** (Fig. 4). Polymorph **1R**, which showed strong fluorescence, had a large distance between the fluorophores (9.441 Å), whereas the fluorophore packing of **1RV** (4.707Å), which had relatively weak fluorescence, was closer. However, the fluorophore distance in **1DO** (6.007 Å) was larger than that of **1RV**, despite the fluorescent quantum yield of **1DO** being much weaker than that of **1RV**. This indicated that the weak fluorescence in **1DO** was dependent on intermolecular interactions other than fluorophore stacking. Differences between the crystal structures of **1DO** and **1Y** were found in the packing of the benzyl groups, although other arrangements were similar (Fig. 5). The benzyl groups in **1DO** formed herring-bone packing, whereas those in **1Y** underwent face-to-face packing. These different packing motifs resulted in slightly different intermolecular interactions in **1DO** and **1Y**. C–H···Cl and C–H···π interactions were observed in the packing of **1DO**, whereas only C–H···Cl interactions were found in that of **1Y** (Table S2). The different packing also had an impact on crystal densities, which were 1.380 g/cm^3 and 1.414 g/cm^3 for **1DO** and **1Y**, respectively (Table 1). In general, fluorescence quenching in the solid state could be attributed to various factors, including loose packing,[20] hydrogen bonding,[21] excimers,[22] low crystallinity,[23] and crystal defects such as impurities.[24] Among them, the weak fluorescence of **1DO** was considered to be caused by its looser packing, because the other factors were not consistent with the observed features of **1DO**, as follows: C–H···π interactions, which were only observed in the crystal structure of **1DO**, are regarded as quite weak hydrogen bonds relative to typical hydrogen bonds that result in fluorescence quenching; the shorter fluorescence lifetime of **1DO** indicated no excimer formation; and no shift and/or modification between the fluorescence spectra of **1DO** and **1Y** showed that crystal imperfections had an insignificant effect on the fluorescence process. Loose packing generally allows molecular motion and increased nonradiative decay rates.[20] Therefore, the weak fluorescence of **1DO** was mainly correlated with the molecular motion caused by the loose packing. Indeed, the FTIR spectrum of **1DO** was slightly different from that of **1Y** in the region from 2800 to 3000 cm^{-1}, particularly the shoulder peak at 2953 cm^{-1} in **1DO** was not found in that of **1Y** (Fig. S6). The band including the peak was assigned

to the C–H stretching vibrations of the methylene moieties of the benzyl groups. This results indicated that the vibration mode of the benzyl groups in **1DO** was more complex than that of **1Y**. The complexity of molecular vibration is considered to be attributed to the loose packing of **1DO**. Loose packing which allowed molecular motion might be correlated with the weak fluorescence of **1DO**, although further studies would be required to clarify the effect of the molecular vibration on the fluorescence decay process.

Similar effects have been observed in the disorder phase of AIE compounds, which showed weak fluorescence due to the molecular motion caused by loose packing.[8b, 25] However, an amorphous solid of **1**, which was regarded as having loose and disordered packing throughout the structure, was found to show intense fluorescence, with a fluorescence quantum yield of 79% (Table 2). The band of infrared spectrum in the C–H stretching vibrations of the methylene moieties of the amorphous solid was distinctive simple spectral shape compared by those of **1DO** and **1Y** (Fig. S6), although the spectral shape of the amorphous solid was different from that of these two polymorphs probably due to the difference in the conformations. This finding suggested that local loose packing induced by the benzyl groups had an essential role in the low fluorescence efficiency of the pyrazine dye, rather than overall loose packing in the solid state.

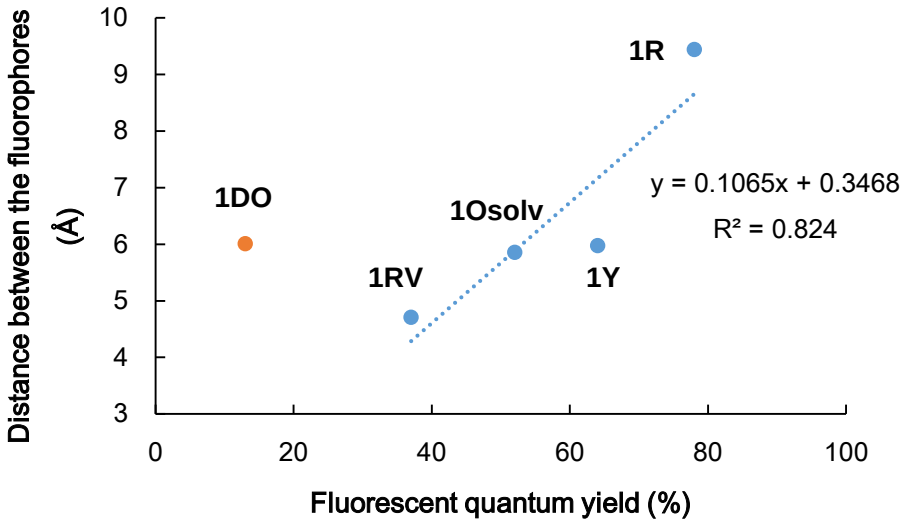

Figure 4. Relationship between fluorophore distance and fluorescent quantum yield. Distance between the fluorophores represents that between the centers of gravity in the fluorophore. The equation in the figure was calculated using **1Y**, **1Osolv**, **1R**, and **1RV**.

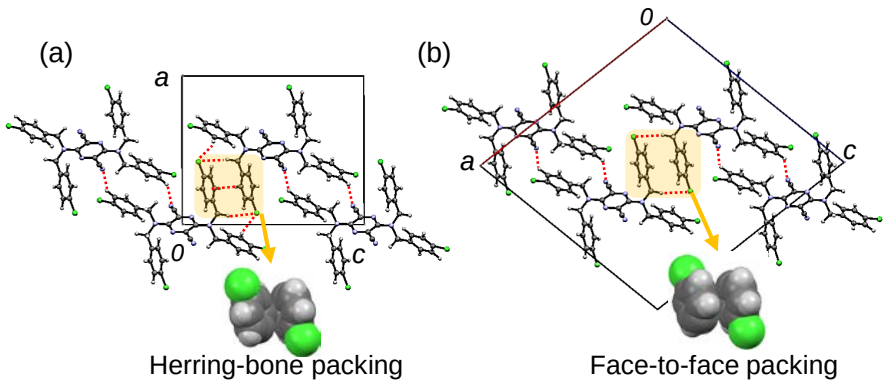

Figure 5. Crystal structures of (a) **1DO** and (b) **1Y**. Yellow square represents the difference in the packing of the benzyl groups: herring-bone packing for **1DO** and face-to-face packing for **1Y**. The red dashed lines represent short contacts.

4. Conclusion

In summary, we identified a packing polymorphism in a new dark orange polymorph of a pyrazine dye. A comparison of the packing polymorphs, and other solid forms, revealed that local loose packing induced by the benzyl groups greatly influenced fluorescence efficiency in the pyrazine dye. This result showed that a benzyl substituent can be used as an effective molecular modification for tuning solid-state fluorescence efficiency.

Acknowledgements

This research was partly supported by the Sasakawa Scientific Research Grant from The Japan Science Society.

References

[1] a) A. Buckley, *Organic Light-Emitting Diodes (OLEDs), Materials, Devices and Applications*, Woodhead publishing, Elsevier Science, 2013; b) H. Fukagawa, T. Shimizu, T. Kamada, S. Yui, M. Hasegawa, K. Morii, T. Yamamoto, *Sci*. *Rep*., **2015**, *5*, 9855; c) D. Yan, D. G. Evans, *Mater*. *Horiz*., 2014, **1**, 46-57.

[2] a) P. An, Z. F. Shi, W. Dou, X. P. Cao, H. L. Zhang, *Org*. *Lett*., 2010, **12**, 4369-4371; b) B. Dong, M. Wang, C. Xu, Q. Feng, Y. Wang, *Cryst*. *Growth Des*., 2012, **12** , 5986-5993; c) D. Yan, G. Fan, Y. Guan, Q. Meng, C. Li, J. Wang, *Phys*. *Chem*. *Chem*. *Phys*., 2013, **15**, 19845-19852; d) Q. Feng, M. Wang, B. Dong, J. He, C. Xu, *Cryst*. *Growth Des*., 2013, **13**, 4418-4427.

[3] a) M. Li, Q. Zhang, J. R. Wanga and X. Mei, *Chem*. *Commun*., 2016, **52**, 11288-11291; b) T. Nicolini, A. Famulari, T. Gatti, J. Martí-Rujas, F. Villafiorita-Monteleone, E. V. Canesi, F. Meinardi, C. Botta, E. Parisini, S. V. Meille, C. Bertarelli, *J*. *Phys*. *Chem*. *Lett*., 2014, **5**, 2171-2176; c) W. Xi, Y. Zhang, B. Chen, X. Gan, M. Fang, J. Zheng, J. Wu, Y. Tian, F. Hao, H. Zhou, *Dyes Pigm.*, 2015, **122**, 31-39.

[4] (a) J. Bernstein, *Polymorphism in Molecular Crystals*, Clarendon Press, Oxford, 2002; (b) A. J. Cruz-Cabeza and J. Bernstein, *Chem*. *Rev*., 2014, **114**, 2170–2191.

[5] a) G. A. Stephenson, T. B. Borchardt, S. R. Byrn, J. Bowyer, C. A. Bunnell, S. V. Snorek, L. Yu, *J*. *Pharm*. *Sci*., 1995, **84**, 1385-1386; b) N. K. Nath, A. Nangia, *Cryst*. *Growth Des*., 2012, **12**, 5411-5425.

[6] a) T. L. Threlfall, *Analyst*, 1995, **120**, 2435-2460; b) J. Bernstein, R. J. Davey, J. O. Henck, *Angew*. *Chem*. *Int*. *Ed*., 1999, **38**, 3440-3461.

[7] a) E. L. Harty, A. R. Ha, M. R. Warren, A. L. Thompson, D. R. Allan, A. L. Goodwin, N. P. Funnell, *Chem*. *Commun*., 2015, **51**, 10608-10611; b) P. S. Hariharan, D. Moon, S. P. Anthony, *J*. *Mater*. *Chem*. *C*, 2015, **3**, 8381-8388.

[8] a) Z. He, L. Zhang, J. Mei, T. Zhang, J. W. Y. Lam, Z. Shuai, Y. Q. Dong, B. Z. Tang, *Chem*. *Mater*., 2015, **27**, 6601-6607; b) A. R. Mallia, R. Sethy, V. Bhat, M. Hariharan, *J*. *Mater*. *Chem*. *C*, 2016, **4**, 2931-2935.

[9] a) Y. Q. Dong, J. W. Y. Lam, B. Z. Tang, *J*. *Phys*. *Chem*. *Lett*., 2015, **6**, 3429-3436; b) Y. Hong, J. W. Y. Lam, B. Z. Tang, *Chem*. *Commun*., 2009, 4332-4353; c) J. Mei, Y. Hong, J. W. Y. Lam, A. Qin, Y. Tang, B. Z. Tang, *Adv*. *Mater*., 2014, **26**, 5429-5479.

[10] Y. Akune, R. Hirosawa, H. Takahashi, M. Shiro, S. Matsumoto, *RSC Adv*., 2016, **6**, 74506-74509.

[11] S. Matsumoto, Y. Uchida, M. Yanagita, *Chem*. *Lett*., 2006, **35**, 654-655.

[12] Y. Akune, H. Gontani, R. Hirosawa, A. Koseki, S. Matsumoto, *CrystEngComm*, 2015, **17**, 5789-5800.

[13] RAPID-AUTO: Rigaku Corporation, 1998, Tokyo, Japan.

[14] SIR2004: M.C. Burla, R. Caliandro, M. Camalli, B. Carrozzini, G.L. Cascarano, L. De Caro, C.

Giacovazzo, G. Polidori and R. Spagna, *J*. *Appl*. *Cryst*., 2005, **38**, 381-388.
[15] SHELXL97: G. M. Sheldrick, *Acta Cryst*., 2008, **A64**, 112-122.
[16] CrysAlisPro version 1.171.39.7e: Rigaku Corporation, Tokyo, Japan
[17] SHELXT version 2014/4: G. M. Sheldrick, *Acta Cryst*., 2014, **A70**, C1437.
[18] CrystalStructure 4.2: Crystal Structure Analysis Package, Rigaku Corporation, Tokyo, Japan.
[19] Mercury 3.8: C. F. Macrae, P. R. Edgington, P. McCabe, E. Pidcock, G. P. Shields, R. Taylor, M. Towler, J. van de Steek, *J*. *Appl*. *Cryst*. 2006, **39**, 453-457.
[20] a) I. Hisaki, E. Kometani, H. Shigemitsu, A. Saeki, S. Seki, N. Tohnai, M. Miyata, *Cryst*. *Growth Des*., 2011, **11**, 5488-5497; b) Y. Mizobe, N. Tohnai, M. Mitata, Y. Hasegawa, *Chem*. *Commun*., 2005, 1839-1841.
[21] a) N. Barman, D. Singha, K. Sahu, *J*. *Phys*. *Chem*. *A*, 2013, **117**, 3945-3953; b) Y. H. Liu, G. J. Zhao, G. Y. Li, K. L. Han, *J*. *Photochem*. *Photobio*. *A*, 2010, **209**, 181-185.
[22] K. Wang, H. Zhang, S. Chen, G. Yang, J. Zhang, W. Tian, Z. Su, Y. Wang, *Adv*. *Mater*., 2014, **26**, 6168-6173.
[23] Y. X. Li, X. F. Yang, J. L. Miao, Z. W. Zhang, G. X. Sun, *CrystEngComm*, 2016, **18**, 2098-2104.
[24] J. Gierschner, L. Lüer, B. Milián-Medina, D. Oelkrug, H. J. Egelhaaf, *J*. *Phys*. *Chem*. *Lett*., 2013, **4**, 2686-2697.
[25] J. Tong, Y. J. Wang, Z. Wang, J. Z. Sun, B. Z. Tang, *J*. *Phys*. *Chem*. *C*, 2015, **119**, 21875-21881.